Accepted refereed manuscript of: Ali F, Cai Q, Hu J, Zhang L, Hoare R, Monaghan SJ & Pang H (2022) In silico analysis of AhyI protein and AI-1 inhibition using N-cis-octadec-9z-enoyl-l-homoserine lactone inhibitor in Aeromonas hydrophila. *Microbial Pathogenesis*, 162, Art. No.: 105356. https://doi.org/10.1016/j.micpath.2021.105356

In silico analysis of AhyI protein and AI-1 inhibition using *N*-cis-octadec-9z-enoyl-l-homoserine lactone inhibitor in *Aeromonas hydrophila*

Farman Ali [2,3 a], Qilan Cai[2,3a], Jialing Hu[1,4], Lishan Zhang[2,3],Rowena Hoare[5], Sean J. Monaghan[5], Huanying Pang[1,4]*

1.College of Fisheries, Guangdong Ocean University, Zhanjiang 524025, China

2. Fujian Provincial Key Laboratory of Agro ecological Processing and Safety Monitoring, College of Life Sciences, Fujian Agriculture and Forestry University, Fuzhou 35002, China

3.Key Laboratory of Crop Ecology and Molecular Physiology (Fujian Agriculture and Forestry University) Fujian Province University, Fuzhou 35002, China

4.Guangdong Provincial Key Laboratory of Pathogenic Biology and Epidemiology for Aquatic Economic Animal, Key Laboratory of Control for Disease of Aquatic Animals of Guangdong Higher Education Institutes, Zhanjiang 524025, China

5. Institute of Aquaculture, University of Stirling, Stirling FK9 4LA, Scotland, UK

* **Correspondence**: phying1218@163.com(H.P.); Tel./Fax: +86-7592339319 (H.P.)

* Authors to whom correspondence should be addressed.

a. These two authors equally contributed to this work.

Abstract: *AhyI* is homologous to the protein *LuxI* and is conserved throughout bacterial species including *Aeromonas hydrophila*. *A. hydrophila* causes opportunistic infections in fish and other aquatic organisms. Furthermore, this pathogen not only poses a great risk for the aquaculture industry, but also for human public health. *AhyI* (expressing acylhomoserine lactone) is responsible for the biosynthesis of autoinducer-1 (AI-1), commonly referred to as a quorum sensing (QS) signaling molecule, which plays an essential role in bacterial communication. Studying protein structure is essential for understanding molecular mechanisms of pathogenicity in microbes.. Here, we have deduced a predicted structure of AhyI protein and characterized its function using *in silico* methods to aid the development of new treatments for controlling *A. hydrophila* infections. In addition to modeling AhyI , an appropriate inhibitor molecule was identified via high throughput virtual screening (HTVS) using mcule drug-like databases. The AhyI-inhibitor N-cis-octadec-9Z-enoyl-L-Homoserine lactone (Could this be abbreviated?) was selected with the best drug score. In order to understand the pocket sites (ligand binding sites) and their interaction with the selected inhibitor, docking (predicted protein binding complex) servers were used and the selected ligand was docked with the predicted AhyI protein model. Remarkably, N-cis-octadec-9Z-enoyl-L-Homoserine lactone established interfaces with the protein via 16 residues (V24, R27, F28, R31, W34, V36, D45, M77, F82, T101, R102, L103, 104, V143, S145, and V168), which are involved with regulating mechanisms of inhibition. These proposed predictions suggest that this inhibitor molecule may be used as a novel drug candidate for the inhibition of auto-inducer-1 (AI-1) activity. The N-cis-octadec-9Z-enoyl-L-Homoserine lactone inhibitor molecule was studied on cultured bacteria to validate its potency against AI-1 production. At a concentration of 40µM, Optimal inhibition efficiency of AI-1 was observed in bacterial culture media. These results suggest that the inhibitor molecule N-cis-octadec-9Z-enoyl-L-Homoserine lactone is a competitive inhibitor of AI-1 biosynthesis.

Keywords: *Aeromonas hydrophila*; LuxI; AhyI; molecular docking; AI-1 biosynthesis; I-TASSER; high throughput virtual screening

1. Introduction

Members of the Aeromonadeacea are opportunistic pathogens that cause infection predominantly in marine organisms, especially fish, but can also cause infection in humans. *Aeromonas hydrophila* is primarily concerned with motile aeromonad septicemia (MAS), a major fish disease challenge affecting the aquaculture industry[1, 2]. During zoonotic infections, *A. hydrophila* is a zoonotic pathogen that causes gastroenteritis ranging from mild enteritis to severe complications of cholera-like- diarrhea. Several fatal *A. hydrophila* induced diseases have also previously been reported such as osteomyelitis, hemolytic uraemic syndrome, peritonitis, and respiratory tract disease[3, 4].

Chemical signals regulate bacterial communication; this mechanism is generally referred to as quorum sensing (QS). QS is a means of communication between cells and enables bacterial species to coordinate mutual behavior in a population density-dependent way.. QS is regulated by diffusible signaling molecules, also known as autoinducers (AIs), such as acylhomoserine lactones (AHLs), typically found in Gram-negative bacteria. QS controls a diverse range of phenotypic traits, such as the formation of biofilms, virulence, motility and plasmid conjugation[5]. The AHLs are the most common type of autoinducers and are synthesized by the homologous LuxI family of AHLs synthases in different bacterial species including as *A. hyrophila*. AhyI is responsible for the synthesis of AHLs. Specificity in signaling activity of AHLs are associated with differences in molecular structure. Although all AHLs retain a uniform homoserine lactone ring, the acyl side chain ranges from four to eighteen carbon atoms in length; the saturation level of the side chain and substitutions of oxo- or hydroxyl- groups at the third carbon plays an important role in the variation of AHL structure[5, 6]. The typical biosynthesis mechanisms of AHLs are shown in Figure 1. This whole system of AHLs production consists of two units, AhyI-type synthase (produces autoinducers-1 in the form of N-acyl homoserine lactone) and AhyR-type (transcriptional regulator) which recognizes the autoinducers and is activated. After its activation, AhyR controls the functions of the AhyI gene and regulates the biosynthesis of N-acyl homoserine lactones (autoinducers). In various Gram-negative bacteria models, variations found in the core QS genes can lead to desensitisation of the QS system[7].The AhyI and AhyR can synthesize and perceive multiple AHLs [8].

There are several molecules found in nature that deactivate QS via blocking different steps of the signaling pathway, and this interference is commonly known as a quorum quenching (QQ). This interference can be controlled by means of:(a) inhibition of AIs synthesis; (b) inhibition of AI

secretion/transport; (c) degradation of AIs by enzymes; (d) sequestration of AIs (e) by antibodies that "mask" and therefore block AI receptors; (f) antagonists of AIs, such as natural or synthetic compounds; (g) inhibition of targets downstream of binding of the AI to the receptor. Furthermore, enzymatically AHLs can be inactivated, and these AHLs QQ enzymes can be categorized into three classes: (a) acylase (amidase or aminohydrolase) that hydrolyses the amide bond between the homoserine lactone ring and acyl chain; (b) lactonase has the capability to open the lactone ring, and (c) oxidoreductase is capable of modifying AHLs by oxi-reduction of the acyl chain at the third carbon without degrading the AHLs. Due to the alarming emergence of antibiotic-resistant bacterial strains, novel antibiotics are demanded for antimicrobial therapy. For this reason QQ research has focused on the finding of new QQ agents to fight against infections [9-14]. In several pathogens, QS regulates virulence factors which can cause disease in host organisms. Therefore, QS blocking can reduce bacterial virulence, providing strategies for new therapies against pathogenic bacteria.

A wide range of QQ enzymes are found in several bacterial species, but there is limited fundamental knowledge regarding the physiological function of these molecules. The LuxI-LuxR QS circuit performs the regulation of lux operon, responsible for producing light in several bacterial species such as *A. fischeri* . In order to understand the function of this protein family, LuxR and LuxI and the corresponding autoinducer (3-oxohexanoyl homoserine lactone, denoted VAI-1), have beenan essential model. LuxR is a receptor for VAI-1 and a transcriptional activator dependent on VAI-1. LuxI directs diffusion into the bacterial envelope for the biosynthesis of N-(3-oxohexanoyl) homoserine lactone (3OC6-HSL)[15, 16]. When 3OC6-HSL/VAI-1 concentration reaches at critical threshold, the DNA binding domain (DBD) transcription activator of the LuxR receptor, activates transcription of lux operon[17, 18]. In addition to the LuxI-LuxR QS, two other QS systems exist, named AinS-AinR and LuxS-LuxP/Q, which indirectly regulate luminescence via modulation of luxR transcription [19]. QS regulates bacterial-pathogen behaviour such as virulence-gene expression, biofilm formation, swarming, antibiotic production, and antibiotic resistance. Regulation of bacterial bioluminescence has previously been studied in two model organisms: *A. fischeri* and *Vibrio campbellii* or *Vibrio harveyi*. Furthermore, 25 bioluminescent species of bacteria have been studied among five genera of three families of the Gamma proteobacteria, such as *Shewanellaceae, Enterobacteriaceae,* and *Vibrionaceae* [20]. These studies demonstrate that QS performs a critical role in the control of lipolytic and virulence pathways. Moreover, the *luxI* homolog *cneI* gene from *Cedeceaneteri* was previously cloned and

subjected to overexpression in an *E.coli* host confirming that this is responsible for the biosynthesis of QS signaling molecules, such as N-butyryl- homoserine lactone (C4-HSL)[21].

The AHL biosynthesis process is catalyzed by the use of AHL synthase LuxI, which plays a role in the transition of the acyl group from the acylated acyl carrier protein (acyl-ACP) to the S-adenosyl-L-methionine amino group (SAM) [22, 23] . The acyl transfer reaction involving an acyl SAM precursor, is reported to occur prior to carboxylate oxygen lactonization to release AHL and Smethylthioadenosine (MTA)[24]. Recently, the LuxI homologue BjaI has now been fully examined to enable the use of acyl-CoA and SAM as substrates, maintaining lactonization to produce the AHL using a preliminary intermediate acyl-SAM[25]. Notably, BjaI's results acknowledged that acyl-CoA may act as BjaI's fatty acyl substrate and could not synthesize AHL in the presence of acyl-ACP. The special AHL biogenesis process indicates that the substrates take on substantially diverse activities from several other LuxI synthases.

Till today, detailed understanding of the structure of AhyI, and the associated binding substrates during the biosynthesis of AHL synthase, is lacking. Furthermore, the functions of each of the amino acid residues during the biosynthesis of ALH remains unknown despite the complete amino acid sequence and conserved residues of AhyI being well documented. Therefore, in this study, a 3D protein model of AhyI of *A.hydrophila* was predicted based on alignment with known homologous structures using homology modeling and fold recognition, or threading methodology. Besides this approach, various computational predictive methods were used, such as sequence analysis, functional annotation, model building, and structure analysis. The goal of this study was to determine and bioinformatically characterise the structure of AhyI of *A.hydrophila*. The subsequent predicted model was validated, and docking of an AI-1 inhibitor was performed using the AhyI model. The efficacy of the AI-1 inhibitor was further verified by *in vitro* methods. These results confirmed that AI-1 QS activity decreased significantly after using an N-cis-octadec-9Z-enoyl-L-Homoserine lactone inhibitor molecule. Overall, these results suggested that this inhibitor molecule reduces the virulence of *A.hyrophila*.

2. Methods

2.1 *In-silico* studies

2.1.1 Bioinformatics analysis of AhyI protein

The UniProt database (Q44058) was used to reterive the amino acids sequences, and sequences were assessed for the prediction of a 3-D structure of the protein while ClustalW was employed for sequence alignment. Both termini, N-terminal, and C-terminal of AhyI protein conatins amino acid sequences important for the prediction of AhyI protein. Based on sequence similarity, structurally homologous sequences were retrieved from protein data bank (PDB). In addition, the Port param tool of ExPASy was used to identify the molecular profile of the AhyI protein sequence. For examining structural properties of the protein, SOPMA, SAPS, and FindMod software packages were used. PSortB and CELLOv2.5 were used to predict the subcellular localization. By using the SignalP4.1 server, signal peptides were analyzed within the amino acid sequence. Predicted Antigenicity of the protein was finally deduced by applying the Antigenic Peptides program.

2.1.2 Structural modeling, validation, and refinement

The AhyI protein homology was exmained by searching against other publically available databases, such as, NCBI and PDB. About 78% homology was identified between the template and the target. Predictions of structural folding was conducted using structural fold recognition techniques, as implemented in the i-TASSER and Phyre2 perdition servers. The existence of additional functional domains was identified by the InterPro protein family database and the Evolutionary classification of protein domains (ECOD) database. Furthermore, i-TASSER was used to gernerate the protein structure, while validation was performed using the SAves server. The quality of the predicted structure was assessed by the QMEAN6 program within the SWISS-MODEL workspace. Ramachandran plots were used for the improvement of protein structure and energy minimization. Finally, the modeled structure was visualized by using of PyMOLv1.7.4.5 program..

2.1.3 Active site, ligand, and ligand binding sites evaluation

The active sites were identified using thecomputed atlas of surface topography of proteins (CASTp). The server locates and measures concave surface regions of modeled proteins. Furthermore, the 3D-ligand binding sites prediction server was employed for the identification of ligand charcteristics and potential binding sites.. Further confirmation of ligand binding sites was achieved using the COACHserver.

2.1.4 High throughput virtual screening and toxicity analysis

High throughput virtual screening (HTVS) was conducted by use of Mcule (https://mcule.com), which is an online drug discovery platform server (Mcule, Inc.PaloAlto, CA 94301, USA). The predicted AhyI protein model was submitted to the mcule database for subsequent ligands searches. During the screening, predicted 3D structures of small molecules are fitted into the binding site of the modeled 3D target structure. Critical interactions of small molecules with the target are predicted based on better (more negative) docking scores and thus ranked higher. Additionally, the OSIRIS property explorer calculator was utilised to optimize the selection of molecules based on their toxicity and other properties such as. mutagenicity, tumorigenicity, and irritant potential, reproductive impact, solubility, molecular weight, hydrophobicity (Clogp value) drug-likeness, and finally the drug score.

2.1.5 Ligand preparation and molecular docking of the target protein

Based on best drug score, N-cis-octadec-9Z-enoyl-L-Homoserine lactone inhibitor was selected for further study. The ligand was extracted in the smile file then transformed into a Mole 2 file format using UCSF chimera, whereby hydrogen was introduced and energy was optimized [26]. After this, using the online Molecular Docking server, docking analyses were carried out[27]. The ligand atoms were supplemented with Gasteiger partial charges. Non-polar atoms of hydrogen were combined and rotatable bonds were established. On the AhyI protein model, docking calculations were performed. Using Auto Dock software, essential hydrogen atoms, Kollman assembled atom type charges, and solvation metrics were applied[28]. The affinity grid was developed using the Autogrid system (Box size: 30x30x30 Å and box center: 60.88 x 60.99x 60.64 for x, y, and z, respectively) with 0.375 Å spacing[29]. For the computation of the van der Waals and the electrostatic terms, the Auto Dock parameter set- and distance-dependent dielectric functions were used, respectively. The Lamarckian genetic algorithm (LGA) and the Solis and Wets local search method were used for docking simulations [30]. The initial position, orientation, and torsion of the molecules of the ligand were randomly set. During docking, all rotatable torsions were recorded. After a maximum of 250,000 energy evaluations, each docking experiment were generated from ten different runs that were configured to terminate.The population size was fixed at 150. A translational step of 0.2 Å, and quaternion and torsion steps of 5 were applied during the analysis.

2.2 In vitro methodology

2.2.1 Bacterial strain and growth conditions

A.hydrophila ATCC 7966 was stored at -80^{0}C in the culture store of laboratory. For culture bacteria were streaked on Luria-Bertani (LB) agar plates, and the next day, a single colony of each bacteria was inoculated into 5 ml LB medium for overnight incubation. For broth culture, bacterial suspension was diluted at1:10 ratios in 100ml LB and grown until an OD600 reached ~1.0. The *E.coli* pSB536 strain was cultured overnight into 1% LB medium with 100µg/ml ampicillin and incubated at 30^{0}C with shaking at 200 rpm. The selected ligand N-cis-octadec-9Z-enoyl-L-Homoserine lactone from the mcule drug database was purchased from Cayman Chemical (1180 E.Ellsworth Road, Ann Arbor, MI 48108, USA).

2.2.2 Bioluminescence assay AI-1 inhibition

Wild type (*A.hydrophila*) strain was cultured overnight at 30^{0}C with and without inhibitor N-cis-octadec-9Z-enoyl-L-Homoserine lactone molecule at various concentrations, 10, 20 and 40µM. Following this, the supernatant was separated by centrifugation at 8000xg for 10 minat 4^{0}C and kept at -20^{0}C for further study. Then, 1ml bacterial culture of reporter strain, *E.coli* pSB536 was centrifuged at 8000xg for 10min, and the supernatant was diluted 1:10 with M9 liquid medium. Furthermore, 100µl of this diluted sample and 100µl M9 liquid medium containing 0.1% *E.coli* pSB536,and were loaded into 96 well plates [31, 32]. Finally, *A.hydrophila* supernatant and the mixture of reporter strain were added along with, and without, the inhibitor molecule at various concentrations, and the AI-1 biosynthesis intensity was measured using a SpectraMax®i3 Molecular device (Molecular Devices, Sunnydale, CA, USA).

2.3 Statistical analysis

Three independent repeats of each experiment were performed, and data were analyzed using GraphPadPrism 7 software. Evaluation of the data was performed via one way analysis of variance (ANOVA) tests, and values are presented with the standard error of the mean (SEM). A *p*-value <0.001 was considered to be statistically significant.

3. Results

3.1 Sequence Analysis, subcellular localization and antigenicity profiling of *A. hydrophila* AhyI

A. hydrophila AhyI sequence analysis revealed a protein length of 207 amino acids, a molecular weight of 23.61kDa, and 3328 total atoms. The hydrophibicity of the protein of-0.229 was

determined by measuring a grand average hydrophobicity (GRAVY) index (Figure 2). Further hydrophobicity of the protein was evaluated using Kyte and Doolittle hydropathy plots.

The functioning of proteins is mainly confined to specific locations. Therefore, protein localization predictions help facilitate understanding of particular cellular mechanisms and pathways, such as disease-associated interactions or QS signaling pathways. The cellular localization of AhyI was predicted ascytoplasmic by using Predict protein and CELLO v2.5 online programs, and the highest cellular localization score of AhyI was 4.847*. Hydrophobic residues such as valine, cysteine, and leucine were found on the surface of the protein and are possible primary components of antigenic determinants. Eight antigenic determinants were predicted in AhyI protein, with an average antigenic propensity of 1.0356 from analysis with the anticipated antigenic peptides tool (Figure 3). These eight antigenic determinants consist of sequence fragments that start and end at different positions: 51–57: DTHWVLI, 62–88: GLCGCIRLLSCAKDYMLPSIFPTALAG, 98-105: WELTRLAI, 118–133: SELTCIIFREVYAFAK, 136-150: GIRELV-AVVSLPVER, 153-160: RRLGLPIE, 163-180: GHRQAVDLGAVRGVGIRF, and 186-196: FARAVGQPLQG. These predicted antigenic sequence segments may play a role in antibody induction.

3.2 *A. hydrophila* AhyI model prediction, refinement and structural analysis

For further, studies at the structural level, homology modeling of the protein was done on the basis of already known protein structure (templates) to predict of 3D-structure of the target sequence. The modeling of the *A. hydrophila* AhyI is more feasible if small variations in protein sequence are present as a small variation is also usually found in the 3D-structure. Differences were found between both the template and the predicted model. The AhyI predicted model contains five beta sheets and has seven alpha-helices. The N-terminus contains long loop residues, and the C-terminus has one short loop residue. The template has 10 alpha helices and five beta-sheets, while the template contains a short loop residue at the N-terminus and a long loop at the C-terminus (Figure 4A and B). Furthermore, the AhyI tertiary structure was accurately predicted by threading methodology using i-TASSER[33-35]. In addition to that, predicted model quality was analyzed using the online package SAVES server [36, 37]. The QMEAN4 server was being used to verify the findings, assess the Ramachandran plot's Psi/Phi values, as well as other quality filtering evaluations against non-redundant protein sets of the data bank. The i-TASSER's prediction analyses of AhyI proteins indicated a higher accuracy than homology modeling.

Furthermore, the AhyI protein model was chosen for energy minimization and model refining based on i-TASSER results and best QMEAN scores (-2.6) and z-score value -5.71.By knowing the overall residue to residue geometry the structural and stereochemical properties of theAhyI model was analyzed using PROCHECK. A Psi/Phi Ramachandran plot was used to assess the quality of the model, and it showed that 77.7% of residues were found in the most favored region, with alternative permitting regions containing 16.8% of residues, and outlier regions with 4.5%, while no single residue was found in non-permitting regions. After observing statistics of the non-bonded interfaces between different atom types, the ERRAT was used to verify the consistency of the AhyI model. Quality evaluation through ERRAT and PROVE indicated that model statistics were suitable and verified the modelling of protein appropriately (Supplemental File 2). Therefore, model validation indicated that the native protein was adequately described by the model.

3.3. Analysis of functional annotation, natural ligand and pocket binding sites/residues within the predicted model of *A. hydrophila* AhyI protein

Predict and ProFun servers were used for functional annotations of the predicted *A. hydrophila* AhyI protein model. These analyses indicated that the AhyI protein participates in various biochemical and biological processes. In particular, AhyI plays a central role in QS, biological regulation, and homeostatic processes and is also involved in biochemical functions linked to the development of biofilm formation, virulence, transferase activity, catalytic activities, and transferring acyl groups. AhyI was also analyzed for its potential to have co-enzyme (COA) ligand pocket binding residues. The coach meta server was used initially to predict and identify the pocket binding residues within the AhyI model and ligand. These binding residues were selected based on high MAMMOTH scores. The interactions between ligand and pocket binding residue are shown in Figure 5 A,B,C and D, which contains the following 16 residues: V24, R27, F28, R31, W34, V36, D45, M77, F82, T101, R102, L103, 104, V143, S145, and V168. Further, we docked S-adenosyl-L-methionine (SAM) and O-(S-fatty acylpantetheine-4’-phosphoryl)-L-serine residue (acyl-[ACP]) into the predicted binding pockets of AhyI protein with binding affinities -8.614 kcal/mol and-7.982 kcal/mol, respectively (Figure 5. E,F).

3.4 Structure-based virtual screening and toxicological analysis

The online Mcule drug database was used for the performing structure based virtual screening. For high throughput virtual screening (HTVs) against the subset of molecules, predictions were made using ligand-binding residues. The maximum identity with *A. hydrophila* AhyI protein 971 HTS ligands was generated based on ligand binding. Moreover, the top ten ligands were selected

for the subsequent study. Property calculator and OSIRIS property calculator were used to assess the toxicological properties of ten selected ligands. Seven non-toxic ligands were found based on toxicological properties out of the ten compounds analysed (Table1).The three toxic-compounds that were predicted were N-(3-chloro-4-methylphenyl)-N'[[1(2thienyl)cyclopropyl]methyl]-oxamide, [(6R)-6hydroxy-1,4-oxazepan-4-yl]-[5(phenylsulfanylmeth-yl)-2-furyl]methanone and4-amino-N-methyl-3-nitro-N-[(1S)-1-(2thi-enyl)ethyl]benzamide. Thus, these molecules were removed for docking studies. The other seven molecules were further screened based on the following parameters, including Mol log P value, Mol log S (solubility), M.W, Mol PSA (A2), drug-likeness, and the drug score (Table2).A molecule was subsequently selected for the docking studies based on the highest drug score.

3.5 Molecular docking

A. hydrophila AhyI protein was docked with selected ligand (N-cis-octadec-9Z-enoyl-L-Homoserine lactone) inhibitor molecule using the online Docking Server. Docking was also performed with all homologous proteins (control). Based on the best binding affinity, docked complexes of protein-ligand were analyzed. The results indicated that an AhyI proteins model had the best binding affinity (-3.53 kcal/mol) with the ligand molecule (Table 3; Figure 6A, B, and C), and the docking results of ligands with homologous proteins were observed (Supplemental File 3).

3.6 *A. hydrophila* AhyI AI-1 biosynthesis inhibition using an N-cis-octadec-9Z-enoyl-L-Homoserine lactone

Bacterial supernatant was used for the detection of AhyI AI-1 activity by performing bioluminescence assay, to assess the effect of AhyI AI-1 QS inhibition on *E.coli* pSB536 and *A.hyrophila*. The inhibitory molecule was applied at different concentrations to the media, and subsequently the inhibitory effect of AhyI AI-1 was analyzed (Figure 7.A). At 40µM concentration of the inhibitory molecule, significant reduction in the activity of AI-1 was observed compared to controls, and treatments with 10 and 20 µM exhibiting lower inhibitory activity of AhyI. The N-cis-octadec-9Z-enoyl-L-Homoserine lactone binds in the pocket sites of the predicted AhyI protein and makes a ligand to the *AhyI*-synthase complex which then blocks the production of QS signaling molecule AI-1, as shown in schematic illustration (Figure 7.B).

4. Discussion

The QS system of signaling is important for gene regulation, producing virulence factors and other pathogenicity-associated activities in pathogenic bacteria such as *V. cholerae* and *A.hydrophila* [1, 38]. Pathogenic bacteria depend on multiple QS signaling molecules, yet the complicated mechanisms through which they regulate gene expression are largely unknown. As opportunistic pathogens, these bacteria interact with other bacteria during infection by perceiving multiple signaling molecules, which is a normal means of communication rather than the exception[2, 39, 40].The intra-species communication is regulated and recognized by acylhomoserine lactone molecules (AHLs) [41-43], and thus, these signals will not interfere with the communication mechanism of other bacterial species[24, 44]. Moreover, the QS circuit of LuxI/R homologous genes have been found in more than a hundred Gram-negative bacterial strains [45], including *SmaIR* in *Serratia marcescens* [46, 47], *CviIR* in *Chromobacterium violaceum*[48, 49], *hanIR* in *Halomonas anticariensis* [50] and *TraIR* of *Agrobacterium tumefaciens* [51] and in AHLs, based on the LuxI/R principle but with moderate modifications. To date, few studies have described the potential for development of QS inhibitor resistance, perhaps as the anti-bacterial mechanism is not bactericidal [52, 53]. When applied at increased doses, QS inhibitors exerts inhibition on growth [54, 55], which can be effectively applied to control infections of marine species, especially in fish. Hence, this report is the first to focus on the structure and functional characterization of AI-1 QS associated AhyI protein of *A.hydrophila* using *in-silico* methods. We show that AhyI protein is reponsible for the synthesis of AHLs/AI-1, and experimentally demonstrate its inhibition by using an inhibitor N-cis-octadec-9Z-enoyl-L-Homoserine lactone. Finally, our results show that bacterial communication can be controlled by inhibition of AI-1 signaling molecules.

The AhyI gene plays a vital role in quorum sensing, and even at high cell densities, produces AI-1 signaling molecules for the intra-species communication [56-58]. For the homology modeling of AhyI structure, sequence alignment of known structures were performed. Homology modeling is merely the modeling method that can provide models with a root mean square error > 2Å. For reliable homology modeling, a basic requirement is to find the similarity between target and template. Therefore we searched for, and found, high sequence identity between target and templates(supplementary file 1, S1.1). The known crystal structures of *Pseudomonas aeruginosa* (PDB ID: 1RO5), *Bradyrhizobium japonicum*, (PDB ID: 5W8A) and *Burkholderia glumae* (PDB ID: 3P2H) were used for homology modeling of *A. hydrophila* AhyI and template (PDB ID: 3P2H) and templates were selected with highest structural similarity and sequence alignment of template and AhyI model (Supplemental File 1). The acyl-homoserine lactone (AHL) synthase LasI is

produced by *P.aeruginosa*, which synthesizes 3-oxo-C12-AHL and from the 3-oxo-C12-acyl-carrier protein (acyl-ACP) and S-adenosyl-L-methionine protein substrates, A V-shaped substrate-binding cleft is created by the LasI six-stranded beta sheet structure. This is knotted by three alpha helices, which leads to a tunnel passing via the enzyme that can support the acyl-ACP acyl chain. In comparison to a restrictive hydrophobic pocket seen from the AHL-synthase EsaI, this tunnel places no obvious constraint on acyl-chain length. *B. japonicum* comprises LuxI-type enzymes that use S -adenosyl-l-methionine and either cellular acyl carrier protein (ACP)-coupled fatty acids or CoA-aryl/acyl moieties as progenitor cells to catalyze the biosynthesis of acyl-homoserine lactones (AHL) signals. QS regulates virulence, motility, and protein secretion in *B. glumae* and protein secretion is controlled by the coupling of N-octanoyl-L-HSL (C8-HSL) to its cognate receptor, TofR. The acyl-HSL synthase TofI synthesizes C8-HSL[59]. In order to deal with predicted models, such models can be divided into three categories from which low accuracy models have target- template alignment identity less than 30%, and therefore should be treated with great care. While medium accurate models are those models obtained via target-template sequence similarity between 30-50% and must have 85% of their C-alpha atoms within 3.5 Å at the right position. This type of model is used for a wide range of biological research applications, like examining ligand binding positions via the design of site-directed mutants with altered binding efficacy, and computational screening of small potential molecules or inhibitors from a variety of databases. The third category of model accuracy depends on high protein sequence similarity which should be more than 50%, with a predicted structure whereby the sequence is capable for comparisons to be made with those structures that have 3 Å resolution - this is considered ideal for ligand docking and drug design computation. If the sequence similarity is more than 90% it is useful for the description of the active site[60].

The comprehensive knowledge of the physicochemical properties of the LuxI/AhyI protein, such as quaternary structure, antigenicity, and structural and functional properties, provides information to determine its role in QS. *In silico* modeling approaches using bioinformatics tools have been used to study several unknown proteins to infer such properties [61]. Current existing knowledge is insufficient for determining the crystal structure of the LuxI/AhyI protein. Here, we have predicted the structure of *A. hydrophila* AhyI protein using *in silico* methods to facilitate further characterization to determine potential drug targets. Furthermore, the data is useful for development of diagnostic markers for hosts infected with the aquatic pathogen, *A. hydrophila. A. hydrophila* AhyI has vital characteristics of communication because of its metal binding, and QS

activity[62]. AhyI protein is a cytoplasmic protein, and its structure was reconstructed and showed low QMEAN4 scores and Z-score values.

Additionally, the validity of the AhyI structure was substantiated with Psi/Phi Ramachandran plots. Therefore, this model has provided alternative drug targets based on the deduced protein structure. This prediction and substantiation of the AhyI structure implied greater than 95% accuracy, inferring a high possibility that the predicted structure is comparable to the native protein. Accurate torsion angle conventions, as are generally present, were observed in the structure and improper dihydral angles that generally are present were also observed. No atoms were missing from the structure, and irregular dihydral angles RMS-scores were within normal ranges. Additionally, all of the essential oxygen atoms were found at the C-terminus.

Most gram-negative bacteria exhibit QS as a vital regulator of bacterial virulence, and the inhibition of the QS molecule is used as an alternative strategy for the control of bacterial infections[63, 64]. It is well reported that the AHL-based QS system of *A.hydrophila* consists of LuxR homologous, AhyR, and LuxI homologous to AhyI, which is responsible for the synthesis of C4-HSL. AhyI mutant strains unable to synthesize C4-HSL consequently fail to produce mature biofilms [62]. Several studies have showed that, by the addition of AHL long chains (i.e.,10-14 HSL) exogenously, the biosynthesis of *Aeromonas* AI-1 system is inhibited leading to reduced biosynthesis of exoproteases[65]. *Vibrio anguillarum* continuously produces 3-oxo-C10-HSL, which reduces the protease activities from *A. salmonicida* and *A. hydrophila* [66]. In addition, synthetic 2(5H)-furanone produced from the marine algae *Deliseapulchra* as a competitive inhibitor of AHL reduced QS activity against C4-HSL and C6-HSL molecules synthesized by aeromonads[67]. For determining *A. hydrophila* AI-1 inhibition, potential and active inhibitors were identified by High throughput virtual screening (HTVS). This was achieved using the Mcule database, with follow-up docking studies performed using online docking programs with an AhyI predicted model and its homologous proteins [68]. A total of 971 hits were obtained based on descending ligand binding affinity with the target protein model. For the evaluation of toxicity of ligands, the top ten ligands were selected. Seven molecules subeqeuntly found as non-toxic were further screened for docking studies. The N-cis-octadec-9Z-enoyl-L-Homoserine lactone molecule was finally chosen for docking based on a higher drug score (0.95). From the dockingevaluation studies, the AhyI predicted model had a better binding affinity and total intermolecualar energy (-3.53Kcal/mol and-7.50Kcal/mol, respectively) with inhibitor N-cis-octadec-9Z-enoyl-L-Homoserine lactone comapred to homologous proteins (Table3). Therefore, these results validated the QS activity of the AI-1 inhibitor N-cis-octadec-9Z-enoyl-L-Homoserine lactone. AI-1

production was also inhibted following analysis of the bacterial strain incubated with 10, 20, and 40 µM concentrations of inhibitor-containing media; the AI-1 biosyhthesis activity of was inhibited at 40µM. This data highlights the potential of this inhibitor as a drug candidate for reducing *A.hydrophila* virulence.

This study expands knowledge on the structure and function of AhyI, a protein integral to quorum sensing activity of gram-negative bacteria. Use of bioinformatics and computational programs facilitate a cost-effective approach to drug discovery. Such comprehensive analysis of conformational changes of proteins, and post-translational modifications are useful to identify important biological targets. Finally, by modeling protein structure, protein-protein interactions, protein- ligands interactions, and binding efficiency of inhibitors through docking studies are made possible .The structural and inhibitor analyses of AhyI protein, using such approaches here, provide a basic framework for the identification of novel drug candidates that can be used to treat bacterial infections caused by *A.hydrophilla*.

5. Conclusions

LuxI/AhyI is responsible for the biosynthesis of quorum sensing signaling AI-1 molecule, which regulates intercommunication in *A. hyrophila* ATCC7966. The 3D- structure of AhyI protein was predicted using in-silico methods, which uncovered the similarity of this structural protein sequence with other homologous proteins. Sixteen pocket sites of protein and ligand-binding residues were predicted(V24, R27, F28, R31, W34, V36, D45, M77, F82, T101, R102, L103, 104, V143, S145, and V168) within the AhyI. By undertaking HTVS the inhibitor molecule N-cis-octadec-9Z-enoyl-L-Homoserine lactone was identified and selected based on the best drug score. This inhibitor molecule was docked with the AhyI model and its homologous proteins and the inhibition was demonstrated on a live *A. hydrophila* strain where AI-1 biosynthesis was significantly reduced using culture media containing 40µM N-cis-octadec-9Z-enoyl-L-Homoserine lactone. These results provide a deeper understanding of AhyI structure and function using state-of-the-art *in silico* tools.

Author Contributions: Huanying Pang and Farman Ali conceived the study. F.A. and Huanying Pang wrote the manuscript; F.A. performed bioinformatics studies, and experiments were done by QilanCai, LishanZhang and Jialing Hudiscussed the results and commented on the main manuscript

and Rowena Hoare, Sean J. Monaghan critically evaluated the study. All authors read and approved the final manuscript.

Funding: This work was funded by the National Key Research and Development Program of China (2018YFD0900501), National Natural Science Foundation of China (No. 31402344, 31670129,32073015), Natural Science Foundation of Guangdong Province (No. 2021A1515011078).

Competing Interests: The authors declare no conflict of interest.

References

[1] Li Z, Wang Y, Li X, Lin Z, Lin Y, Srinivasan R, et al. The characteristics of antibiotic resistance and phenotypes in 29 outer-membrane protein mutant strains in *Aeromonas hydrophila*. Environmental microbiology. 2019;21:4614-28.
[2] Sun L, Yao Z, Guo Z, Zhang L, Wang Y, Mao R, et al. Comprehensive analysis of the lysine acetylome in *Aeromonas hydrophila* reveals cross-talk between lysine acetylation and succinylation in LuxS. Emerging microbes & infections. 2019;8:1229-39.
[3] Yao Z, Guo Z, Wang Y, Li W, Fu Y, Lin Y, et al. Integrated Succinylome and Metabolome Profiling Reveals Crucial Role of S-Ribosylhomocysteine Lyase in Quorum Sensing and Metabolism of *Aeromonas hydrophila*. Molecular & Cellular Proteomics. 2019;18:200-15.
[4] Parker JL, Shaw JG. *Aeromonas spp*. clinical microbiology and disease. Journal of Infection. 2011;62:109-18.
[5] Williams P, Winzer K, Chan WC, Camara M. Look who's talking: communication and quorum sensing in the bacterial world. Philosophical Transactions of the Royal Society B: Biological Sciences. 2007;362:1119-34.
[6] Whitehead NA, Barnard AM, Slater H, Simpson NJ, Salmond GP. Quorum-sensing in Gram-negative bacteria. FEMS microbiology reviews. 2001;25:365-404.
[7] Papenfort K, Bassler BL. Quorum sensing signal–response systems in Gram-negative bacteria. Nature Reviews Microbiology. 2016;14:576.
[8] Williams P. Quorum sensing, communication and cross-kingdom signalling in the bacterial world. Microbiology. 2007;153:3923-38.
[9] Chen F, Gao Y, Chen X, Yu Z, Li X. Quorum quenching enzymes and their application in degrading signal molecules to block quorum sensing-dependent infection. International journal of molecular sciences. 2013;14:17477-500.
[10] Guendouze A, Plener L, Bzdrenga J, Jacquet P, Rémy B, Elias M, et al. Effect of quorum quenching lactonase in clinical isolates of *Pseudomonas aeruginosa* and comparison with quorum sensing inhibitors. Frontiers in microbiology. 2017;8:227.
[11] Utari PD, Setroikromo R, Melgert BN, Quax WJ. PvdQ quorum quenching acylase attenuates *Pseudomonas aeruginosa* virulence in a mouse model of pulmonary infection. Frontiers in Cellular and Infection Microbiology. 2018;8:119.
[12] Murugayah SA, Gerth ML. Engineering quorum quenching enzymes: progress and perspectives. Biochemical Society Transactions. 2019;47:793-800.
[13] Grandclément C, Tannières M, Moréra S, Dessaux Y, Faure D. Quorum quenching: role in nature and applied developments. FEMS microbiology reviews. 2015;40:86-116.
[14] LaSarre B, Federle MJ. Exploiting quorum sensing to confuse bacterial pathogens. Microbiol Mol Biol Rev. 2013;77:73-111.
[15] Langebrake JB, Dilanji GE, Hagen SJ, De Leenheer P. Traveling waves in response to a diffusing quorum sensing signal in spatially-extended bacterial colonies. Journal of theoretical biology. 2014;363:53-61.
[16] Dilanji GE, Langebrake JB, De Leenheer P, Hagen SJ. Quorum activation at a distance: spatiotemporal patterns of gene regulation from diffusion of an autoinducer signal. Journal of the American Chemical Society. 2012;134:5618-26.

[17] TEICHMANN S. FAMILIES OF SEQUENCE-SPECIFIC DNA-BINDING DOMAINS IN TRANSCRIPTION FACTORS ACROSS THE TREE OF LIFE. PROTEIN FAMILIES. 2014:383.
[18] Lixa C, Mujo A, Anobom CD, Pinheiro AS. A structural perspective on the mechanisms of quorum sensing activation in bacteria. Anais da Academia Brasileira de Ciências. 2015;87:2189-203.
[19] Lukjancenko O, Ussery DW. Vibrio chromosome-specific families. Frontiers in microbiology. 2014;5:73.
[20] Dunlap PV, Urbanczyk H. Luminous bacteria. The Prokaryotes: Prokaryotic Physiology and Biochemistry. 2013:495-528.
[21] Tan K-H, How K-Y, Tan J-Y, Yin W-F, Chan K-G. Cloning and Characterization of the Autoinducer Synthase Gene from Lipid-Degrading Bacterium *Cedecea neteri*. Frontiers in microbiology. 2017;8:72.
[22] Moré MI, Finger LD, Stryker JL, Fuqua C, Eberhard A, Winans SC. Enzymatic synthesis of a quorum-sensing autoinducer through use of defined substrates. Science. 1996;272:1655-8.
[23] Schaefer AL, Val DL, Hanzelka BL, Cronan JE, Greenberg EP. Generation of cell-to-cell signals in quorum sensing: acyl homoserine lactone synthase activity of a purified *Vibrio fischeri* LuxI protein. Proceedings of the National Academy of Sciences. 1996;93:9505-9.
[24] Watson WT, Minogue TD, Val DL, Von Bodman SB, Churchill ME. Structural basis and specificity of acyl-homoserine lactone signal production in bacterial quorum sensing. Molecular cell. 2002;9:685-94.
[25] Dong S-H, Frane ND, Christensen QH, Greenberg EP, Nagarajan R, Nair SK. Molecular basis for the substrate specificity of quorum signal synthases. Proceedings of the National Academy of Sciences. 2017;114:9092-7.
[26] Goddard TD, Huang CC, Ferrin TE. Visualizing density maps with UCSF Chimera. Journal of structural biology. 2007;157:281-7.
[27] Bikadi Z, Hazai E. Application of the PM6 semi-empirical method to modeling proteins enhances docking accuracy of AutoDock. Journal of cheminformatics. 2009;1:15.
[28] Halgren TA. Merck molecular force field. I. Basis, form, scope, parameterization, and performance of MMFF94. Journal of computational chemistry. 1996;17:490-519.
[29] Morris GM, Goodsell DS, Halliday RS, Huey R, Hart WE, Belew RK, et al. Automated docking using a Lamarckian genetic algorithm and an empirical binding free energy function. Journal of computational chemistry. 1998;19:1639-62.
[30] Solis FJ, Wets RJ-B. Minimization by random search techniques. Mathematics of operations research. 1981;6:19-30.
[31] Brackman G, Celen S, Baruah SK, Bossier P, Van Calenbergh S, Nelis H, et al. AI-2 quorum sensing inhibitors affect the starvation response and reduce virulence in several *Vibrio* species, most likely by interfering with LuxPQ. MICROBIOLOGY-SGM. 2009;155:4114-22.
[32] Vilchez R, Lemme A, Thiel V, Schulz S, Sztajer H, Wagner-Döbler I. Analysing traces of autoinducer-2 requires standardization of the *Vibrio harveyi* bioassay. Analytical and bioanalytical chemistry. 2007;387:489-96.
[33] Yang J, Yan R, Roy A, Xu D, Poisson J, Zhang Y. The I-TASSER Suite: protein structure and function prediction. Nature methods. 2015;12:7.
[34] Roy A, Kucukural A, Zhang Y. I-TASSER: a unified platform for automated protein structure and function prediction. Nature protocols. 2010;5:725.
[35] Kelley LA, Sternberg MJ. Protein structure prediction on the Web: a case study using the Phyre server. Nature protocols. 2009;4:363.
[36] Pontius J, Richelle J, Wodak SJ. Deviations from standard atomic volumes as a quality measure for protein crystal structures. Journal of molecular biology. 1996;264:121-36.
[37] Lüthy R, Bowie JU, Eisenberg D. Assessment of protein models with three-dimensional profiles. Nature. 1992;356:83.
[38] Bardill JP, Zhao X, Hammer BK. The Vibrio cholerae quorum sensing response is mediated by Hfq-dependent sRNA/mRNA base pairing interactions. Molecular microbiology. 2011;80:1381-94.
[39] Wang Y, Wang X, Ali F, Li Z, Fu Y, Yang X, et al. Comparative extracellular proteomics of Aeromonas hydrophila reveals iron-regulated secreted proteins as potential vaccine candidates. Frontiers in immunology. 2019;10:256.
[40] Li W, Yao Z, Sun L, Hu W, Cao J, Lin W, et al. Proteomics analysis reveals a potential antibiotic cocktail therapy strategy for Aeromonas hydrophila infection in biofilm. Journal of proteome research. 2016;15:1810-20.
[41] Yao Y, Martinez-Yamout MA, Dickerson TJ, Brogan AP, Wright PE, Dyson HJ. Structure of the Escherichia coli quorum sensing protein SdiA: activation of the folding switch by acyl homoserine lactones. Journal of molecular biology. 2006;355:262-73.
[42] Bottomley MJ, Muraglia E, Bazzo R, Carfì A. Molecular insights into quorum sensing in the human pathogen Pseudomonas aeruginosa from the structure of the virulence regulator LasR bound to its autoinducer. Journal of Biological Chemistry. 2007;282:13592-600.
[43] Chen G, Swem LR, Swem DL, Stauff DL, O'Loughlin CT, Jeffrey PD, et al. A strategy for antagonizing quorum sensing. Molecular cell. 2011;42:199-209.

[44] Gould TA, Schweizer HP, Churchill ME. Structure of the *Pseudomonas aeruginosa* acyl-homoserinelactone synthase LasI. Molecular microbiology. 2004;53:1135-46.
[45] Case RJ, Labbate M, Kjelleberg S. AHL-driven quorum-sensing circuits: their frequency and function among the Proteobacteria. The ISME Journal. 2008;2:345.
[46] Salini R, Pandian SK. Interference of quorum sensing in urinary pathogen *Serratia marcescens* by Anethum graveolens. Pathogens and disease. 2015;73.
[47] Thomson N, Crow M, McGowan S, Cox A, Salmond G. Biosynthesis of carbapenem antibiotic and prodigiosin pigment in *Serratia* is under quorum sensing control. Molecular microbiology. 2000;36:539-56.
[48] McClean KH, Winson MK, Fish L, Taylor A, Chhabra SR, Camara M, et al. Quorum sensing and *Chromobacterium violaceum*: exploitation of violacein production and inhibition for the detection of N-acylhomoserine lactones. Microbiology. 1997;143:3703-11.
[49] Deryabin D, Inchagova K. Inhibitory effect of aminoglycosides and tetracyclines on quorum sensing in Chromobacterium violaceum. Microbiology. 2018;87:1-8.
[50] Tahrioui A, Quesada E, Llamas I. The hanR/hanI quorum-sensing system of Halomonas anticariensis, a moderately halophilic bacterium. Microbiology. 2011;157:3378-87.
[51] Zhu J, Winans SC. Autoinducer binding by the quorum-sensing regulator TraR increases affinity for target promoters in vitro and decreases TraR turnover rates in whole cells. Proceedings of the National Academy of Sciences. 1999;96:4832-7.
[52] Defoirdt T, Boon N, Bossier P. Can bacteria evolve resistance to quorum sensing disruption? PLoS pathogens. 2010;6:e1000989.
[53] García-Contreras R, Maeda T, Wood TK. Can resistance against quorum-sensing interference be selected? The ISME journal. 2016;10:4.
[54] García-Contreras R, Peréz-Eretza B, Jasso-Chávez R, Lira-Silva E, Roldán-Sánchez JA, González-Valdez A, et al. High variability in quorum quenching and growth inhibition by furanone C-30 in *Pseudomonas aeruginosa* clinical isolates from cystic fibrosis patients. Pathogens and disease. 2015;73.
[55] Quave CL, Lyles JT, Kavanaugh JS, Nelson K, Parlet CP, Crosby HA, et al. Castanea sativa (European Chestnut) leaf extracts rich in ursene and oleanene derivatives block *Staphylococcus aureus* virulence and pathogenesis without detectable resistance. PLoS One. 2015;10:e0136486.
[56] Xavier KB, Bassler BL. LuxS quorum sensing: more than just a numbers game. Current opinion in microbiology. 2003;6:191-7.
[57] Plummer PJ. LuxS and quorum-sensing in *Campylobacter*. Frontiers in cellular and infection microbiology. 2012;2.
[58] Plummer P. LuxS and quorum-sensing in *Campylobacter*. Frontiers in cellular and infection microbiology. 2012;2:22.
[59] Hubbard T, Blundell T. Comparison of solvent-inaccessible cores of homologous proteins: definitions useful for protein modelling. Protein engineering. 1987;1:159-71.
[60] Marsden RL, Orengo CA. Target selection for structural genomics: an overview. Structural Proteomics: High-Throughput Methods. 2008:3-25.
[61] Ali F, Yao Z, Li W, Sun L, Lin W, Lin X. In-Silico Prediction and Modeling of the Quorum Sensing LuxS Protein and Inhibition of AI-2 Biosynthesis in *Aeromonas hydrophila*. Molecules. 2018;23:2627.
[62] Lynch MJ, Swift S, Kirke DF, Keevil CW, Dodd CE, Williams P. The regulation of biofilm development by quorum sensing in *Aeromonas hydrophila*. Environmental microbiology. 2002;4:18-28.
[63] Talagrand-Reboul E, Jumas-Bilak E, Lamy B. The social life of Aeromonas through biofilm and quorum sensing systems. Frontiers in microbiology. 2017;8:37.
[64] Churchill ME, Chen L. Structural basis of acyl-homoserine lactone-dependent signaling. Chemical reviews. 2010;111:68-85.
[65] Swift S, Lynch MJ, Fish L, Kirke DF, Tomás JM, Stewart GS, et al. Quorum sensing-dependent regulation and blockade of exoprotease production in *Aeromonas hydrophila*. Infection and immunity. 1999;67:5192-9.
[66] Li X. The impact of cell-to-cell signaling and host cues on the virulence of *Vibrio anguillarum* towards gnotobiotic sea bass (Dicentrarchus labrax) larvae: Ghent University; 2014.
[67] Ponnusamy K, Paul D, Kim YS, Kweon JH. 2 (5H)-Furanone: a prospective strategy for biofouling-control in membrane biofilm bacteria by quorum sensing inhibition. Brazilian Journal of Microbiology. 2010;41:227-34.
[68] Grosdidier A, Zoete V, Michielin O. EADock: docking of small molecules into protein active sites with a multiobjective evolutionary optimization. Proteins: Structure, Function, and Bioinformatics. 2007;67:1010-25.

Figure legends

Figure 1. The auto inducer dependent QS circuit of gram-negative (*Aeromonas hydrophila*) bacteria. AhyI-type synthase homologs produce AHLs signaling molecules consisting of a homoserine lactone ring molecule which binds with an acyl side chain via amide bonds and substitutions. AhyR-type homologs recognize AHLs, the transcriptional regulators consist of two domains: an N-terminal that adhere to AHL and a C-terminal domain identifies a DNA sequence. The protein structures in this diagram are indicated; these are the predicted models of AhyI and AhyR of *A. hydrophila*.

Figure 2. Doolittle hydropathy plot presenting the hydrophilic nature of the *A. hydrophila* AhyI protein.

Figure 3. Profile and antigenic determinants of *A. hydrophila* AhyI. Grey lines show the positions of eight antigenic determinants within the AhyI protein.

Figure 4.(A) *A. hydrophila* AhyI predicted model. (B) AhyI template. Red indicates alpha-helices, yellow indicates sheets, and green indicates loops.

Figure 5. Prediction of pocket binding sites within the *A. hydrophila* AhyI protein and interaction of predicted natural ligand. (A) Predicted AhyI protein pockets, (B)represents the COA ligand binds with AhyI pockets, (C) A COA-ligand (Co-enzyme A in ring structure (red) and pocket binding residues are labeled with amino acid names and numbers, (D) 3-D hydrophobicity view of AhyI-COA complex. **(E,F)** hydrophobicity view of *S*-adenosyl-L-methionine (SAM) and butyryl-acyl carrier protein (acyl-[ACP]) with the pockets of AhyI protein, respectively.

Figure 6.(A) *A. hydrophila* AhyI protein docked with ligand (B) the schematic illustration of interaction (C) 3D-hydrophobicity overview of N-cis-octadec-9Z-enoyl-L-Homoserine lactone inhibitor molecule with protein.

Figure 7. AI-1 inhibitor molecule inhibits the *A. hydrophila* AhyI AI-1 biosynthesis (A) Measurement of AI-1 activity using reporter strain *E.coli* pSB536 which was incubated with culture supernatant of *A. hydrophila* in the presence and absence of AI-1 inhibitor molecule. The bioluminescence measurement was analyzed six hours after the addition of the inhibitor molecule. Bioluminescence was lower than that of the untreated control ($p < 0.001$ ***, and $p < 0.05$ *). (B) Schematic illustration of AI-1 inhibition. The error bars calculated by standard error of the mean (SEM).

658 **Table 1.**Properties of the ten selected molecules. Molecules were removed based on
659 toxic effects (represented in bold format).

Structural Formulae	Name of Molecules	Effects on Reproduction	Irritant to Skin	Mutagenic	Carcinogenic
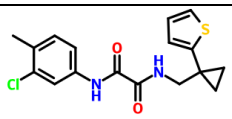	**N-(3-chloro-4-methylphenyl)-N'[[1(2thienyl) cyclopropyl]methyl]-oxamide**	**Mild risk of reproductive effect**	**Mild risk of irritant**	**Non**	**--**
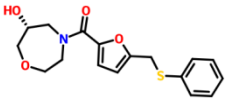	**[(6R)-6 hydroxy-1,4-oxazepan-4-yl]-[5-(phenylsulfanylmethyl)-2-furyl]methanone**	**--**	**Medium risk of irritant**	**--**	**Non**
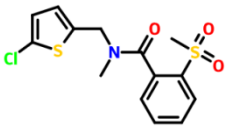	N-[(5-chloro-2-thienyl)methyl]-N-methyl-2-methylsulfonyl-benzamide	Non	Non	Non	Non
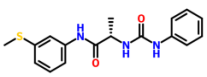	(2S)-N-(3methylsulfa-nylphenyl)-2-(phenyl-carbamoylamino)propanamide	Non	Non	Non	Non
	(S)-N-(oxotetrahydro-furan-3-yl)oleamide /(N-cis-octadec-9Z-enoyl-L-Homoserine lactone)	Non	Non	Non	Non
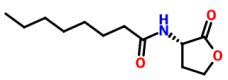	(S)-N-(2-oxoTetra-hydrofuran-3-yl)octanamide	Non	Non	Non	Non
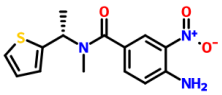	**4-amino-N-methyl-3-ni tro-N-[(1S)-1-(2 thi-enyl)ethyl]benzamide**	**Reproductive Effects**	**Also mild irritant**	**--**	**Mild tumorigenic detected**
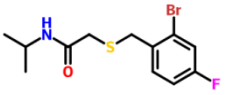	2-[(2-bromo-4-fluoro-phenyl)methylsulfanyl]-N-isopropyl-acetamide	Non	Non	Non	Non
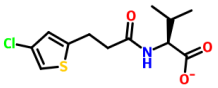	(2S)-2-[3-(4-chloro-2-thienyl)propanoylamino]-3-methylbutanoic	Non	Non	Non	Non
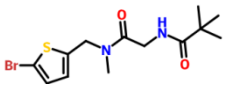	N-[2-[(5-bromo-2-thienyl)methyl-methyl-amino]-2-oxo-ethyl]-2,2-dimethyl-propanamide	Non	Non	Non	Non

660

661

662

Table 2. Screening of seven non-toxic molecules. A molecule was selected for docking based on high drug scores (shown in bold).

Chemical structure	Molecules	Mol.Wt	MolLogS (Solubility)	Mol LogP	Drug likeliness	Mol PSA(A^2)	Drug Score
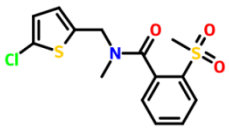	N-[(5-chloro-2-thienyl)methyl]-N-methyl-2-methylsulfonyl-benzamide	343.8	-4.45	2.33	-0.02	47.16	0.29
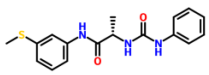	(2S)-N-(3methylsulfa-nylphenyl)-2-(phenyl-carbamoylamino)propanamide	329.4	-5.11	3.17	-1.35	56.39	0.75
	**(S)-N-(oxotetrahydro-furan-3-yl)oleamide /(N-cis-octadec-9Z-enoyl-L-Homoserine lactone)**	**365.5**	**-6.81**	**6.22**	**0.29**	**46.98**	**0.95**
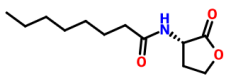	(S)-N-(2-oxoTetra-hydrofuran-3-yl)octanamide	227.3	-3.12	1.86	-0.39	46.98	0.29
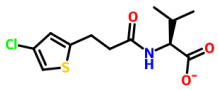	(2S)-2-[3-(4-chloro-2-thienyl)propanoylamino]-3-methylbutanoic	288.7	-3.96	2.49	-1.19	53.49	0.42
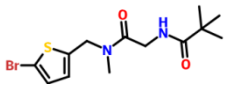	N-[2-[(5-bromo-2-thienyl)methyl-methyl-amino]-2-oxo-ethyl]-2,2-dimethyl-propanamide	347.2	-3.52	2.31	0.20	41.84	0.90
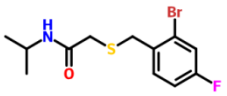	2-[(2-bromo-4-fluoro-phenyl)methylsulfanyl]-N-isopropyl-acetamide	320.2	-4.62	3.53	0.09	23.68	0.79

Table 3. The calculation of energy binding affinity and intermolecular energy of *A hydrophila* AhyI proteins with ligand, identified using the docking server.

Protein PDB: ID and Species Name	Energy Binding Affinity	Total Intermolecular Energy
AhyI (predicted model) *A.hydrophila*	-3.53Kcal/mol	-7.50Kcal/mol
AHL synthase (3P2H) *B.glumae* (control)	-4.82 Kcal/mol	-9.44 Kcal/mol
AHL synthase (5W8A) *B.japonicum*(control)	-6.22 Kcal/mol	-11 Kcal/mol
AHL synthase (1RO5) *P.aeruginosa* (control)	-2.84 Kcal/mol	-5.74Kcal/mol

Figure.1

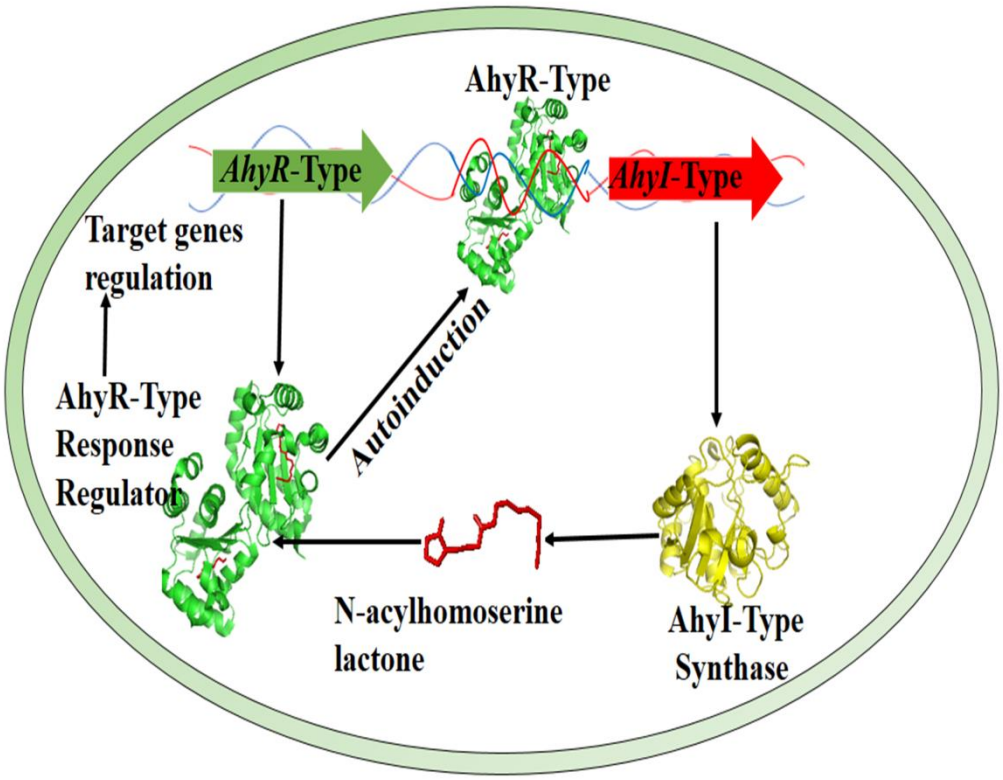

671

672

673 **Figure.2**

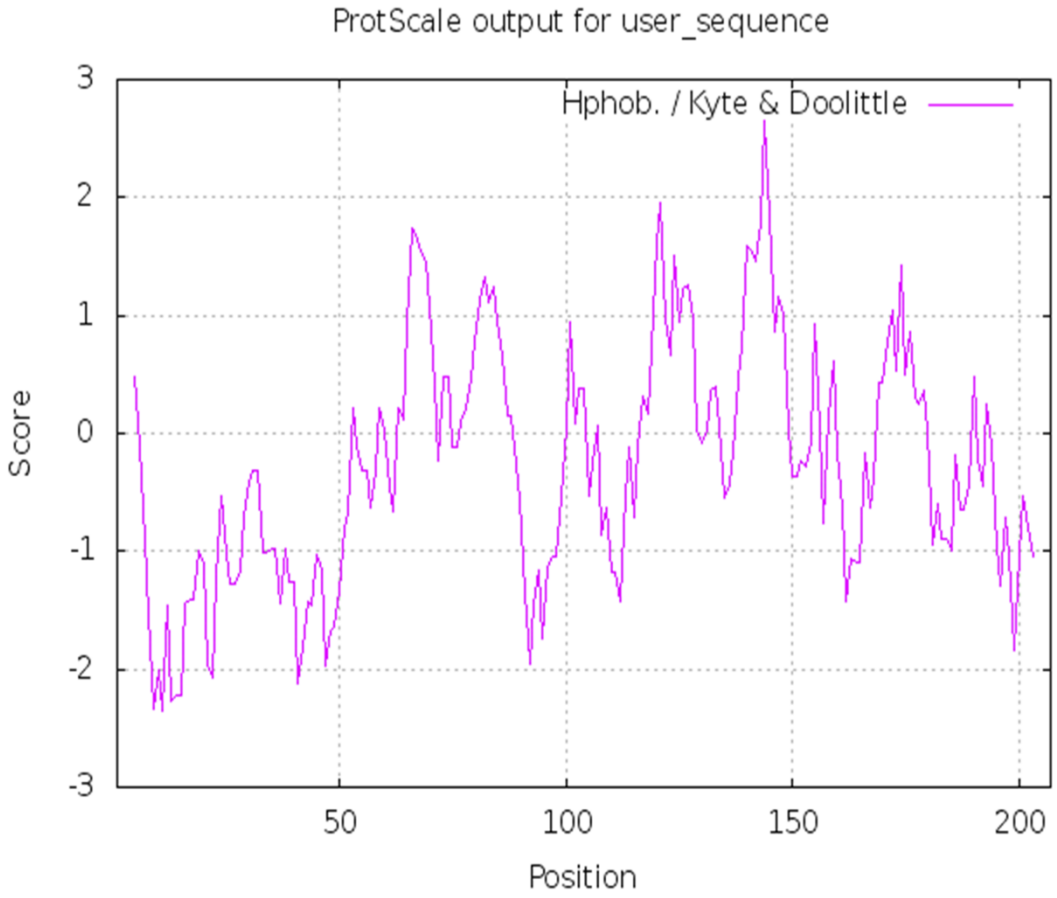

674

675 **Figure.3**

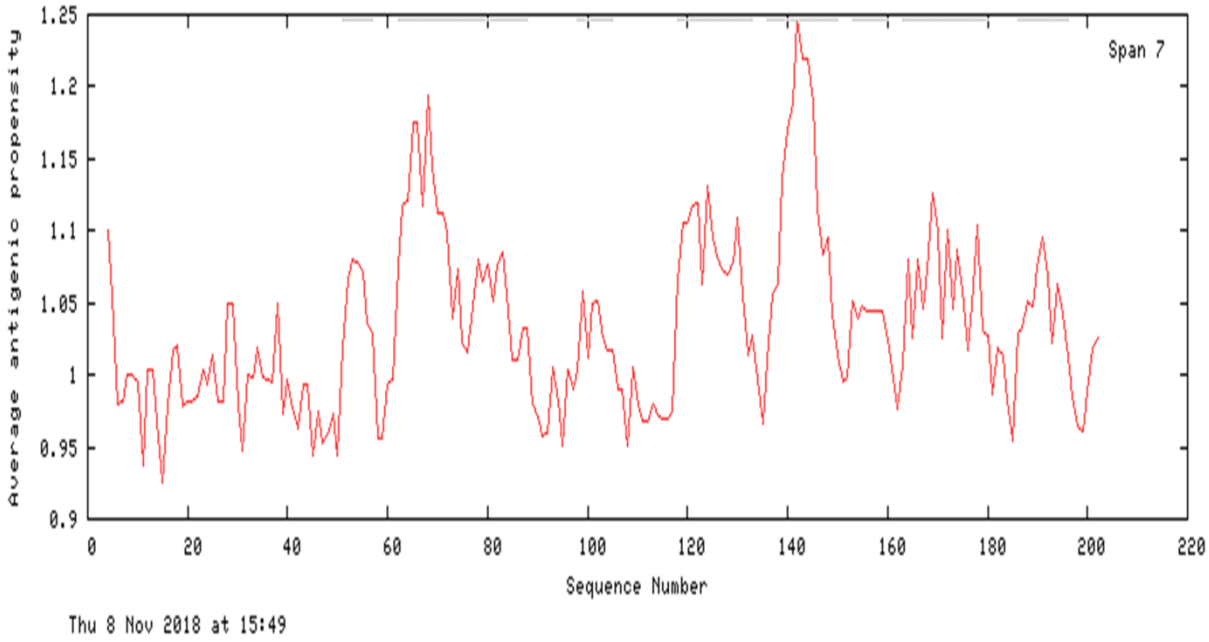

676

677 **Figure.4**

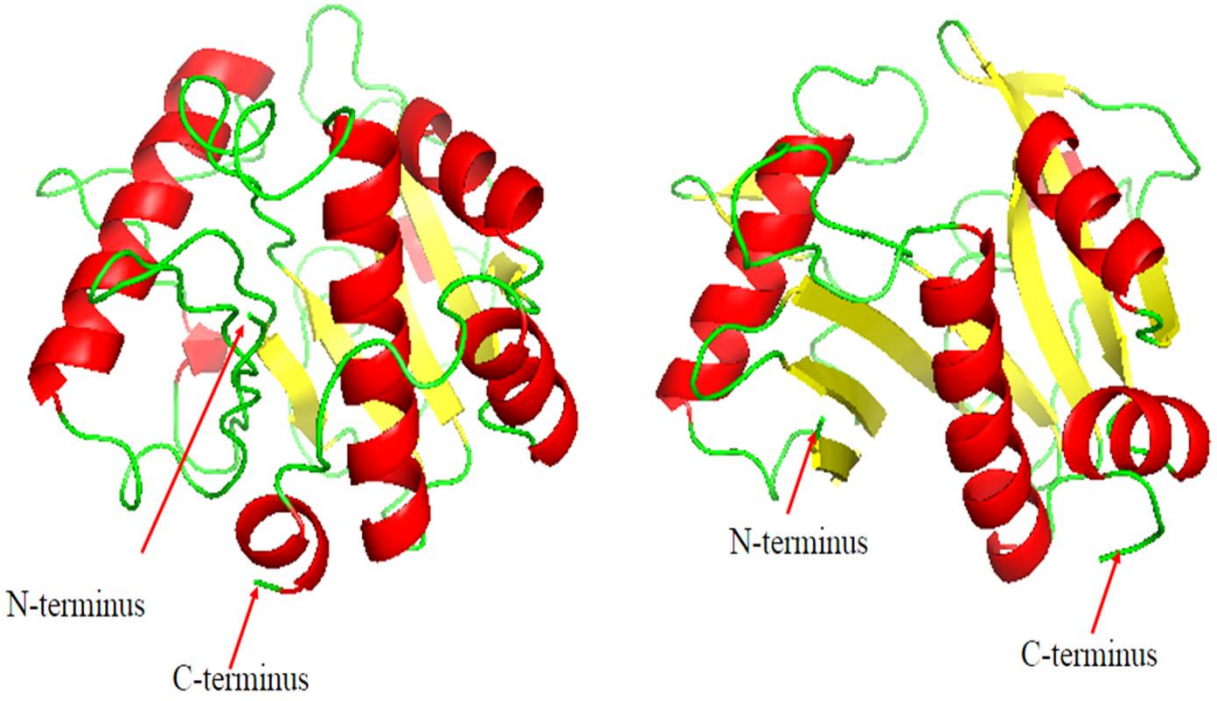

678

679 **Figure.5**

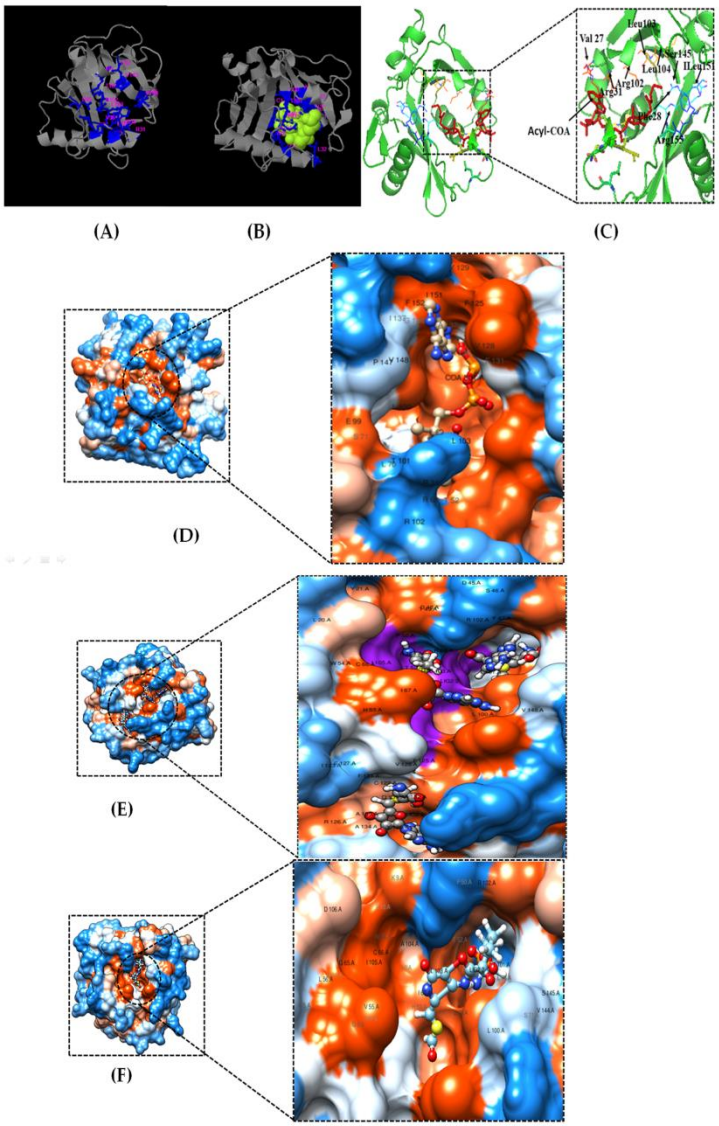

680

681 **Figure. 6**

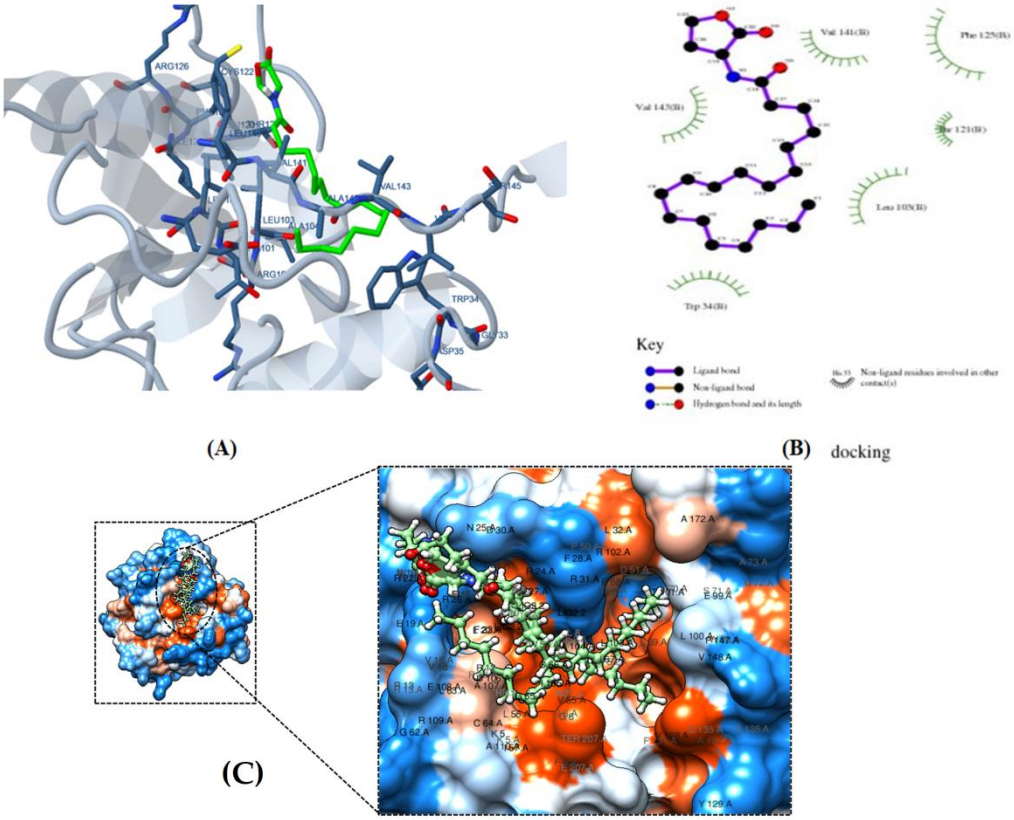

682

683

684 **Figure.7**

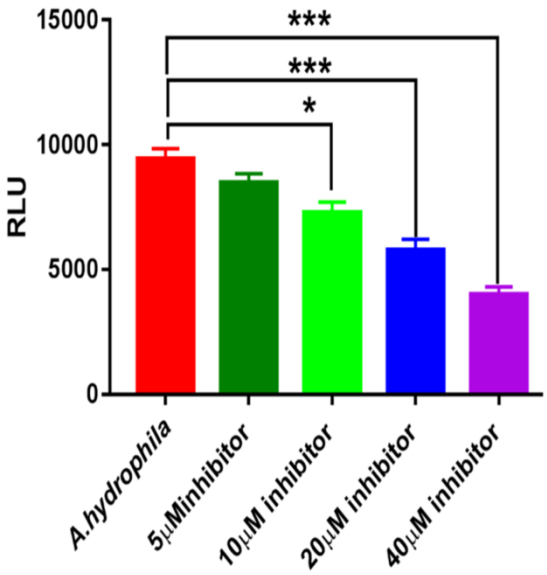
15000
10000
5000
0
RLU
***
***
*
A.hydrophila
5μMinhibitor
10μM inhibitor
20μM inhibitor
40μM inhibitor

(A)

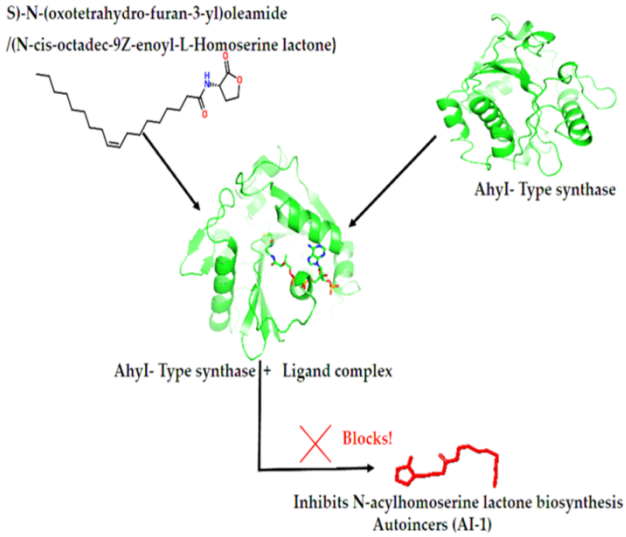
S)-N-(oxotetrahydro-furan-3-yl)oleamide
/(N-cis-octadec-9Z-enoyl-L-Homoserine lactone)
AhyI- Type synthase
AhyI- Type synthase + Ligand complex
Blocks!
Inhibits N-acylhomoserine lactone biosynthesis
Autoincers (AI-1)

(B)

685